

**SYNTHESIS AND THERMAL CONDUCTIVITY OF COPPER
NANOPARTICLE ENCAPSULATED BY GRAPHENE**

by

SEBASTIAN DAYOU

**Thesis submitted in fulfillment of
the requirements for the degree of
Doctor of Philosophy**

July 2017

ACKNOWLEDGEMENTS

First and foremost I would like to glorify The Almighty Lord for His grace and rich blessings.

A PhD Degree is designed to be the sole contribution of one individual. Even so, there are many people who have been of great help to me all through the journey. It is my pleasure to acknowledge them. Special thanks to my wife, parents and family members for their ever-lasting love, prayers, patience and support that have kept me motivated throughout my PhD endeavor.

I wish to express my deepest gratitude and appreciation to my supervisors, Professor Dr. Abdul Rahman Mohamed and Dr. Brigitte Vigolo for their time and effort despite their busy schedule to offer feedbacks, advices, suggestions and discussions throughout the research. These individuals have been the main catalyst and contributor of this work. Their teachings and experiences shared are invaluable and someone whom I look up to for qualities of a great researcher. Most importantly, I would like to thank them for the privilege given to me for a 2 months research attachment stint at Group 205 of Institut Jean Lamour in Université de Lorraine, Nancy, France. It has been of great help in achieving the objectives my research work. It is also a pleasure to be able meet with some nice individuals and visiting some beautiful places in Nancy, definitely an experience that I will never forget.

Throughout my research works, I have the honor to work with some enthusiastic individuals who had helped me in my research. I would like to acknowledge the work by researchers from Institut Jean Lamour, Nancy, France: Dr. Jaafar Ghanbaja for HRTEM observations and analysis; Dr. Ghouti Medjahdi for XRD analysis; and Dr. Alexandre Desforges for analysis on graphene synthesis rate; as well as the staffs from Science and Engineering Research Center, USM: En.

Mohd. Zharif Ahmad Thirmizir and En. Mohd Azrul Bin Abd Aziz for HRTEM and SEM observations; Pn. Hariy Pauzi for XPS characterizations; and Pn. Ee Bee Choo from School of Physics, USM for FESEM characterizations. I am also grateful to the Dean, Deputy Deans and all the technical staffs in School of Chemical Engineering, USM for their technical assistance. My colleagues from ARM Graphene group also deserve special mention for all the discussion and suggestions that has helped to shape the idea and opening pathways for this research work. Also, I would like to thank all my friends and members of Penang Adventist Hospital Church, for their friendship and prayers.

Last but not least, the financial support of the Ministry of Higher Education of Malaysia (MyBrain15 Program) as well as the research funding from the IReC grant (1002/PJKIMIA/910404) and Science Fund grant (Project No.: 03-01-05-SF0659) are greatly acknowledged.

Thank you very much!

TABLE OF CONTENTS

| | Page |
|---|------|
| ACKNOWLEDGEMENTS | ii |
| TABLE OF CONTENTS | iv |
| LIST OF TABLES | vii |
| LIST OF FIGURES | viii |
| LIST OF ABBREVIATIONS | xi |
| LIST OF SYMBOLS | xiv |
| ABSTRAK | xv |
| ABSTRACT | xvii |
| | |
| CHAPTER ONE: INTRODUCTION | |
| 1.1 Graphene | 1 |
| 1.2 Solar thermal energy storage | 3 |
| 1.3 Problem statements | 7 |
| 1.4 Objectives | 10 |
| 1.5 The scope of study | 10 |
| 1.6 Organization of thesis | 11 |
| | |
| CHAPTER TWO: LITERATURE REVIEW | |
| 2.1 Growth of graphene by chemical vapor deposition | 13 |
| 2.1.1 Growth of graphene on metal particles by CVD | 16 |
| 2.1.2 Effect of catalyst and CVD conditions | 22 |
| 2.2 Towards high yield and low cost production of graphene by CVD | 25 |
| 2.3 Materials for high conductivity enhancement of phase change materials | 28 |

| | | |
|-------|--|----|
| 2.3.1 | Nanomaterials as thermal conductivity enhancer | 29 |
| 2.3.2 | Percolation network for effective thermal conductivity enhancement | 37 |
| 2.4 | Summary | 40 |

CHAPTER THREE: MATERIALS AND METHODS

| | | |
|----------|--|----|
| 3.1 | Materials and chemicals | 42 |
| 3.2 | Experimental rig of the chemical vapor deposition system | 43 |
| 3.3 | Experimental steps | 46 |
| 3.3.1 | Catalyst preparation | 47 |
| 3.3.2 | Synthesis of graphene by chemical vapor deposition | 48 |
| 3.3.3 | Separation of graphene | 48 |
| 3.3.4 | Characterization techniques | 49 |
| 3.3.4(a) | X-ray fluorescence spectrometry | 49 |
| 3.3.4(b) | Scanning electron microscopy | 49 |
| 3.3.4(c) | X-ray diffraction | 50 |
| 3.3.4(d) | X-ray photoelectron spectroscopy | 50 |
| 3.3.4(e) | Transmission electron microscopy | 51 |
| 3.3.4(f) | Raman spectroscopy | 51 |
| 3.3.4(g) | Thermogravimetric analysis | 52 |
| 3.3.4(h) | Thermal conductivity measurements | 53 |

CHAPTER FOUR: RESULTS AND DISCUSSION

| | | |
|-----|--|----|
| 4.1 | Catalyst preparation for CVD growth of graphene from CuO-MgO | 54 |
| 4.2 | Growth of graphene | 61 |

| | | |
|-------|--|----|
| 4.2.1 | Morphological and structural characteristics of the grown carbon nanomaterials | 62 |
| 4.2.2 | Carbon nanotubes produced as by-product | 69 |
| 4.2.3 | Content of graphene determined by TGA | 73 |
| 4.2.4 | Effect of copper composition on the quantity of grown graphene | 78 |
| 4.2.5 | Growth mechanism of graphene | 79 |
| 4.2.6 | Efficiency, rate and cost of graphene synthesis | 85 |
| 4.3 | Thermal conductivity of heat storage material added with graphene on CuO-MgO | 90 |

CHAPTER FIVE: CONCLUSION AND RECOMMENDATIONS

| | | |
|-----|-----------------|----|
| 5.1 | Conclusion | 96 |
| 5.2 | Recommendations | 98 |

REFERENCES 101

APPENDICES

Appendix A : Preliminary work using Cobalt as catalyst

Appendix B : Calculation sample to deposit 5 mol.% of Cu on MgO

Appendix C : Preparation of Fe-MgO

Appendix D : Calculation on the amount of produced graphene over the catalyst particles, growth efficiency and rate per synthesis from Table 4.3.

Appendix E : Calculation on the production price of graphene based on the price of the initial reactants used (Table 4.4)

Appendix F : Growth of CNT on Co-MgO catalyst

LIST OF PUBLICATION

LIST OF TABLES

| | | Page |
|-----------|---|------|
| Table 2.1 | Previous works on the synthesis of graphene by CVD using a particle-based metal catalyst | 16 |
| Table 2.2 | CVD conditions and graphene production yield from previous works | 26 |
| Table 2.3 | Compilation of studies from the reviews done by Khodadadi et al. (2013), Kibria et al. (2015) and Gasia et al. (2016) related to the use of various nanomaterials for thermal conductivity enhancement in TES materials | 30 |
| Table 3.1 | List of chemicals and reagents | 42 |
| Table 3.2 | Major components in the CVD experimental rig system | 44 |
| Table 4.1 | Elemental analysis of impurities in raw MgO and as-prepared catalyst | 55 |
| Table 4.2 | The content of graphene produced by CuO-MgO (250 mg) under the flow of CH ₄ (50 mL/min), H ₂ (100 mL/min) and N ₂ (100 mL/min). | 86 |
| Table 4.3 | Comparison of graphene growth yields with previous works reported in literature | 86 |
| Table 4.4 | Calculation of the production price of graphene | 89 |

LIST OF FIGURES

| | | Page |
|------------|---|------|
| Figure 1.1 | Schematic diagram of a CSP power plant (SolarReserve, 2016). | 5 |
| Figure 2.1 | Typical images of graphene under (a) TEM and (b) SEM. Inset in (a) showing crumpled paper which represent the morphology of crumpled graphene structure (Monthieux et al., 2017; Wang et al., 2009a). | 19 |
| Figure 2.2 | Schematic diagram of steps in CNT growth mechanism by CVD: (a) dissociation of hydrocarbon, (b) graphene cap growth, and (c) tube elongation forming CNT. | 21 |
| Figure 2.3 | Schematic diagram of GNP-SWNT network in the epoxy matrix (Yu et al., 2008). | 38 |
| Figure 3.1 | Schematic diagram of the CVD experimental rig system. | 44 |
| Figure 3.2 | Flowchart of the overall experimental activities in the present study. | 47 |
| Figure 4.1 | Elemental mapping of the prepared CuO-MgO catalyst: (a) SEM image, and EDX map of (b) Cu, (c) Mg, (d) O. | 57 |
| Figure 4.2 | XPS spectra at Cu2p energy region of the prepared catalyst. | 59 |
| Figure 4.3 | XRD patterns of the prepared CuO-MgO catalyst. Inset is the enlarged view of the peaks within the dotted region. Assignment of the diffraction peaks: red for MgO, green for CuO and *for pigeonite ((Ca,Mg,Fe)(Mg,Fe)Si ₂ O ₆). | 60 |
| Figure 4.4 | TEM images of sample after CVD reaction done at 950 C, 30 min. | 63 |
| Figure 4.5 | Typical TEM and HRTEM images of graphene after the CVD synthesis done at 950°C for 60 min (a & b), 980°C for 30 min (c & d) and 1000°C for 30 min (e & f). | 63 |
| Figure 4.6 | Typical HRTEM images focused on the edges of the commonly encountered graphene after the CVD synthesis at 1000 °C for 30 min. | 64 |
| Figure 4.7 | Observation under (a) SEM and (b) TEM of sample after the CVD synthesis done at 1050 °C for 30 min. | 65 |
| Figure 4.8 | Typical SEM images showing the two forms of graphene after solubilization of MgO with CVD reaction done at | 66 |

950°C, 60 min (a and c), 1000°C, 30 min (b and d).

| | | |
|-------------|---|----|
| Figure 4.9 | TEM micrograph of the (a) graphenic material after CVD synthesis at 1000 °C for 30 min, and (b) the corresponding SAED pattern; reflections (002) and (101) from the graphitic-ordered structure of the grown multi-layer grapheme correspond to $d_{002} = 0.335$ nm and $d_{101} = 0.203$ nm. | 68 |
| Figure 4.10 | HRTEM image of graphene after CVD synthesis at 950 °C for 60 min. Inset showing the corresponding (a) FFT and (b) inverse FFT with enhanced lattice images at the selected area (white square) of the few layer graphene structure. | 69 |
| Figure 4.11 | TEM images on sample after solubilization of MgO with CVD reaction done at 950°C for 60 min (a and b) and 1000 °C for 30 min (c and d) showing noticeable presence of CNTs (white arrow) as by-product. Images (b) and (d) are the enlarged view of white square region in (a) and (c), respectively. | 70 |
| Figure 4.12 | TEM and SEM images showing CNTs on bare MgO, after the CVD reaction done at 950°C for 30 min (a, b and c), 950°C for 60 min (d, e and f) and at 950°C for 60 min as iron (10 mol.%) is deposited on MgO (g and h). | 71 |
| Figure 4.13 | Typical Raman spectra of the samples after growth on the bare MgO powder after CVD at (i) 950°C, 30 min, (ii) 950°C, 60 min and (iii) 1000°C, 30 min. | 72 |
| Figure 4.14 | (a) TGA curves and (b) the corresponding differential thermogravimetric profiles (dTG) of the as-synthesized sample grown from CuO-MgO catalyst under various CVD reaction conditions. | 75 |
| Figure 4.15 | (a) TGA and dTG profile under He environment of the as-produced samples after CVD at 1000 °C for 30 min and (b) the corresponding mass spectroscopy data. | 76 |
| Figure 4.16 | dTG profile of 5 mol.% Cu-MgO tested under CVD temperature of 1000 °C for 30 min and 10 mol.% Fe-MgO tested at 950 °C for 60 min. | 77 |
| Figure 4.17 | TGA curves of the as-synthesized sample grown from various composition of CuO-MgO catalyst under CVD reaction of 950 °C for 60 min | 78 |
| Figure 4.18 | a) TEM micrograph of an encapsulated copper oxide particle at the surface of MgO (CVD reaction done at 950°C for 60 min) and b) corresponding FFT analysis. | 81 |

| | | |
|-------------|--|----|
| Figure 4.19 | XRD patterns before (as-prepared catalyst) and after the CVD reaction done at different conditions: at 950°C for 30 and 60 min, at 980°C for 30 min and at 1000°C for 30 min. Assignment of the diffraction peaks: red for MgO, green for CuO, orange for Cu ₂ O and blue for Cu. Cu _{Kα} radiation at $\lambda = 1.54056 \text{ \AA}$. | 81 |
| Figure 4.20 | XPS spectra of (a) Cu2p and (b) O1s of the CuO-MgO prepared catalyst and samples after the CVD reaction done at 950°C for 60 min, at 980°C for 30 min and at 1000°C for 30 min. | 83 |
| Figure 4.21 | Graphene growth mechanism. Creation of oxygen vacancy due to reduction phenomenon by hydrogen. At these defective sites, favored dehydrogenation of methane gases. Facile formation of graphene layers. | 84 |
| Figure 4.22 | SEM images of the surface of pellets after uniaxial compression of (a) graphene-CuO-MgO and salt and (b) MgO, graphene and salt. | 91 |
| Figure 4.23 | (a) Thermal conductivity and (b) specific heat of samples with various compositions and preparation method. | 93 |

LIST OF ABBREVIATIONS

| | |
|-----------------|--------------------------------------|
| μm | Micron |
| 3D | Three-dimensional |
| Ar | Argon |
| at. | Atomic |
| C | Carbon |
| CH_4 | Methane |
| CNF | carbon nanofiber |
| CNT | Carbon nanotube |
| Co | Cobalt |
| Co-MgO | Cobalt supported on MgO |
| CSP | Concentrated Solar Power |
| Cu | Copper |
| CuCl_2 | Copper chloride |
| Cu-MgO | Copper supported on MgO |
| CuO | Copper oxide |
| CuO-MgO | Copper oxide supported on MgO |
| CVD | Chemical vapor deposition |
| dTG | Differential thermogravimetric |
| DWNT | Double-walled nanotube |
| EDS | Energy dispersive X-ray spectrometry |
| eV | ElectronVolt |
| Fe | Iron |
| Fe-MgO | Iron supported on MgO |

| | |
|---------------------|--|
| FFT | Fast Fourier transform |
| g | Gram |
| GNP | Graphene nanoplatelet |
| h | Hour |
| H | Hydrogen |
| H ₂ | Hydrogen gas |
| He | Helium |
| HRTEM | High-resolution transmission electron microscope |
| HTF | Heat transfer fluid |
| kV | KiloVolt |
| Mg | Magnesium |
| mg | Milligram |
| Mg(OH) ₂ | Magnesium hydroxide |
| MgO | Magnesium oxide |
| min | Minute |
| mL | Milliliter |
| mm | Millimeter |
| mol. | Mole |
| MPa | MegaPascal |
| MWNT | Multi-walled nanotube |
| N | Nitrogen |
| N/A | Not applicable |
| N ₂ | Nitrogen gas |
| Ni | Nickel |
| nm | Nanometer |

| | |
|------|------------------------------------|
| O | Oxygen |
| PCM | Phase change material |
| PMMA | Poly(methyl methacrylate) |
| ppm | parts per million |
| PV | Photovoltaic |
| R&D | Research and development |
| RBM | Radial breathing mode |
| RT | Room temperature |
| SAED | Selected area electron diffraction |
| sccm | Standard cubic centimeter |
| SEM | Scanning electron microscope |
| SWNT | Single-walled nanotube |
| TEM | Transmission electron microscope |
| TES | Thermal energy storage |
| TGA | Thermogravimetric analysis |
| TPS | Transient plane source |
| USD | United States Dollar |
| v/v | Volume/volume |
| vol. | Volumetric |
| wt. | Weight |
| XPS | X-ray photoelectron spectroscopy |
| XRD | X-ray diffraction |
| XRF | X-ray fluorescence |

LIST OF SYMBOLS

| | |
|-----|----------------------|
| % | Percent |
| " | Inch |
| ° | Degree |
| °C | Degree Celsius |
| Å | Angstrom |
| d | D-spacing |
| m/z | Mass-to-charge ratio |
| z | Charge |
| θ | Theta |
| λ | Wavelength |

SINTESIS DAN KEBERALIRAN HABA NANOZARAH KUPRUM YANG DIBALUT OLEH GRAFENA

ABSTRAK

Kaedah mudah aplikasi pemendapan wap kimia (CVD) telah digunakan untuk mensintesis grafena yang dimangkin oleh kuprum yang disokong di atas MgO. Penggunaan komposit grafena-CuO-MgO (iaitu produk selepas proses CVD) sebagai bahan tambah untuk meningkatkan keberaliran haba dalam bahan penyimpan tenaga haba juga dikaji. CuO-MgO telah disediakan dengan memendap kuprum berzarah nano di atas permukaan serbuk MgO dengan menggunakan teknik impregnasi. Kajian melalui mikroskop pengimbas elektron digandingkan dengan teknik serakan tenaga sinar-X menunjukkan yang zarah-zarah kuprum berskala nano telah dimendapkan secara seragam di atas permukaan MgO. Pertumbuhan grafena dilakukan pada tekanan atmosfera di dalam sebuah reaktor unggun tetap yang mendarat tanpa adanya langkah penurunan yang khusus sebelum proses tindakbalas CVD; oleh yang demikian, zarah kuprum berada dalam keadaan oksida semasa proses pertumbuhan grafena berlaku. Mekanisme pertumbuhan grafena di atas kuprum oksida telah dikaji dengan teliti dengan menggunakan spektroskopi fotoelektron sinar-X dan pembelauan sinar-X. Buat pertama kalinya dibuktikan dengan jelas bahawa kuprum (5 mol.%) dalam bentuk oksida, secara efektif memangkin pertumbuhan grafena yang berlapis nipis apabila tindakbalas CVD dijalankan pada suhu 950 °C selama 60 min, 980 °C selama 30 min and 1000 °C selama 30 min di bawah aliran gas metana (50 mL/min), nitrogen (100 mL/min) dan hidrogen (100 mL/min). Mekansime pertumbuhan grafena diusulkan mengikut turutan berikut: (i) CuO mengalami proses penurunan oleh gas hidrogen yang

mengakibatkan terbentuknya kekosongan kedudukan atom oksigen pada permukaan, (ii) penyah-hidrogenan terhadap metana pada kedudukan tersebut, dan (iii) seterusnya pembentukan jaringan grafitik yang menjadikan lapisan-lapisan grafena. Berdasarkan cara alternatif, terus dan tepat menerusi analisis termogravimetri, kandungan grafena yang tinggi berjaya dihasilkan (lingkungan 9.6 % dalam peratusan jisim) apabila tindakbalas CVD dijalankan pada suhu 1000 °C selama 30 minit. Berbanding dengan kaedah lain yang sedia ada, kaedah mensintesis grafena yang digunakan di dalam kajian ini adalah lebih cekap (125 % dalam peratusan jisim terhadap pemangkin) dan memberikan kadar pertumbuhan grafena yang tinggi (42 mg/ min/ g pemangkin) serta dihasilkan pada kos yang lebih rendah disebabkan oleh penggunaan bahan mentah yang lebih murah. Bahan yang dihasilkan selepas CVD (iaitu grafena beserta CuO-MgO) berpotensi tinggi untuk digunakan dalam aplikasi penyimpanan tenaga haba kerana ia dijangka boleh meningkatkan mutu kebolehaliran haba dengan wujudnya rangkaian terus sesama juzuk-juzuk unsur (iaitu antara grafena, CuO dan MgO) bagi saluran pengaliran haba. Berdasarkan data kajian yang diperolehi daripada kaedah sumber alihan tarahan, bahan in memberikan 51% peningkatan terhadap keberaliran haba terhadap bahan penyimpan haba.

SYNTHESIS AND THERMAL CONDUCTIVITY OF COPPER NANOPARTICLE ENCAPSULATED BY GRAPHENE

ABSTRACT

A facile chemical vapor deposition (CVD) method was used to synthesize graphene, which was catalyzed by copper supported on MgO. The use of graphene-CuO-MgO composite (i.e. the product after CVD) as additive for thermal conductivity enhancement in thermal energy storage material was also investigated. CuO-MgO was prepared by depositing 5 mol. % of copper nanoparticle on MgO powder using an impregnation technique. Investigation under scanning electron microscope coupled with energy dispersive X-ray spectrometry revealed that the copper nanoparticles were evenly deposited on the surface of MgO powders. The CVD process was carried out at atmospheric pressure in a horizontal fixed bed reactor without a dedicated reduction step prior to CVD reaction process; hence copper nanoparticle was in its oxidized state during the growth process of graphene. The mechanism by which graphene grows on copper oxide was deeply investigated by X-ray photoelectron spectroscopy and X-ray diffraction. For the first time, it was unambiguously proven that copper oxide (5 mol.%) efficiently catalyze the growth of few- and multi-layered graphene when the CVD reaction was conducted at 950 °C for 60 min, 980 °C for 30 min and 1000 °C for 30 min under the flow of methane (50 mL/min), nitrogen (100 mL/min) and hydrogen (100 mL/min). The mechanism of graphene growth was proposed in the following order: (i) reduction process of CuO by hydrogen that creates oxygen vacancies on the surface, (ii) methane dehydrogenation on the oxygen vacancy site and (iii) subsequent construction of graphitic network forming graphene layers. Based on the result from an alternative,

direct and accurate approach of thermogravimetric analyses, high content of graphene was able to be produced (around 9.6 wt. %) when the CVD reaction was conducted at 1000°C for 30 min. Compared to the existing methods, this corresponds to a high efficiency (125 wt.%) and growth rate of graphene (42 mg/ min/ g of catalyst), produced at a considerably lower cost since cheaper raw materials were utilized. The as-produced material after CVD (i.e. graphene together with CuO-MgO) has high potential to be used in thermal energy storage applications due to the expected high thermal conductivity enhancement it could offer from the establishment of direct contact between the constituents, i.e. graphene, CuO and MgO, forming an interconnected network for heat conduction pathway. Based on the thermal investigation using a transient plane source method, 51% enhancement to the thermal conductivity of the thermal storage material was recorded.

CHAPTER ONE

INTRODUCTION

This chapter presents the background of the current research work which covers topics such as graphene, renewable energy and thermal energy storage for solar applications. Separate sections are assigned for each of these topics. Then, the motivations of the present work are expressed after identifying the current issues faced. A set of objectives are outlined and the scope of the present study is described. Finally, the organization of chapters in this thesis is given.

1.1 Graphene

Graphene, a one-atom thick film of sp^2 -bonded carbon atom with hexagonal arrangement, has ignited strong interest from the scientific community ever since its discovery in 2004 by Professor Andre Geim and Professor Konstantin Novoselov from the University of Manchester, United Kingdom. This discovery won them the Nobel Prize in Physics 2010 for “groundbreaking experiments regarding the two-dimensional material graphene”. The high attention toward graphene is due to its unique properties that have not been previously observed in other nanomaterials such as outstanding electronic properties (Novoselov et al., 2005; Bonaccorso et al., 2010), superior optical (Bonaccorso et al., 2010; Li et al., 2009a) and mechanical (Lee et al., 2008) properties as well as exceptional ability to conduct electricity (Li et al., 2009a) and heat (Ghosh et al., 2008; Balandin et al., 2008). The combination of these incredible properties allows it to be used, in the future, in myriad applications such as sensors and biosensors (Liu et al., 2015; Green and Norton, 2015), bioengineering (Gao and Duan, 2015), biomedical (Liu et al., 2013; Krishna et al.,

2013), composite materials (Wang et al., 2014a), energy technology (Hu et al., 2015; Wang and Liu, 2015) and solar cells (Das et al., 2014).

The discovery of graphene had brought forth new area of carbon nanomaterials after carbon nanotubes (CNTs). Since its discovery, research and technology innovations based on graphene has been rising exponentially. The number of patent applications and granted patents on graphene has even surpassed that of CNTs in 2013 and 2014 (Zurutuza and Marinelli, 2014). Based on the latest data on the worldwide patent landscape from the Informatics team at the UK Intellectual Property Office (2015), there are over 25,000 published patents related to graphene from 2005 to 2014 as compared to only 50 patents application submitted prior to that. It is natural to expect growth in graphene innovations in 2015 and beyond considering the observed upward trend.

Despite many significant breakthroughs in the laboratories, the commercial adoption of graphene is deemed slow (Zurutuza and Marinelli, 2014; Levchenko et al., 2016) and many of its touted application is yet to be fully materialized. One of the main reasons for this is related to the problem of high production cost for graphene, thus limiting their scalability from the laboratory tested techniques (Raccichini et al., 2014; Novoselov et al., 2012). In this scenario, closing the gap between laboratory-scale research and practice applications has been one of the main agenda among research scientists. This effort is important in order to meet its increasing demand for the coming years. Graphene markets is projected to grow from USD 20 million in 2014 to more than USD 390 million in 2024 (ReportBuyer, 2015). One major sector that graphene is expected to be heavily invested upon is in the area of renewable energy (Novoselov et al., 2012).

1.2 Solar thermal energy storage

A shift towards green energy and power generation from renewable resources has garnered increasing interest worldwide (IRENA, 2015) due to great concern over the depletion of fossil fuels and also the climate change and greenhouse emissions brought by the usage of these conventional energy sources. In this situation, harnessing power from natural resources such as solar, wind, hydro, ocean, geothermal and biomass for renewable energy is undoubtedly the best option because it can offer sustainable energy generation and certainly can minimize the negative impact to the environment. Rapid deployment of technologies based on renewable energies such as solar photovoltaic (PV) technologies (Radomes Jr and Arango, 2015; Ghafoor and Munir, 2015), solar thermal concentrating solar power (CSP) (Nonnenmacher et al., 2016), on- and off- shore wind energy (Zhao et al., 2015), hydropower (Hennig, 2016) and bio-energy (Guo et al., 2015) has been established around the world and they are projected to grow substantially in the coming years (IRENA, 2015) to meet the increasing energy demand.

Globally, there is a good mix of the technologies based on renewable energy that are currently being heavily utilized for energy generation such as solar photovoltaic in Germany, solar CSP in Spain, on-shore wind power in the United States, hydropower in China, biomass in Finland and geothermal energy in Indonesia. The type of technology being deployed is inherently governed by specific geographical factors whereas different parts of the world vary by the different types of natural abundance and energy requirements. However, the current global energy provider is still dominated by fossil fuels, while renewable energy accounts to around 13.5% of the global energy demand (Sahoo, 2016). The main drawback of renewable energy sources is that they are naturally intermittent and this may generate high

fluctuations of power output that would hinder power network stability and reliability (Luo et al., 2015). The use of energy storage is very important to deal with this issue in order to make these renewable sources more stable and dependable for practical applications (Daim et al., 2012). This is done by storing the excess energy being generated and then released for later use when needed (Hadjipaschalis et al., 2009). Therefore, technologies based on energy storage will play a crucial role in achieving a solid, efficient and cost-effective power distribution from renewable energy towards becoming the main energy contributors for the society's energy supply (Kousksou et al., 2014).

Solar energy has been touted as the type of renewable energy with the brightest future due to its supreme resource potential compared to other renewable alternatives (Lewis, 2016; Khan and Arsalan, 2016). In the past decade, research and development (R&D) efforts and deployment activities concerning the utilization of solar energy has been intensified. Solar-derived PV and CSP are the two most prominent technologies in this sector (Lewis, 2016). PV dominates CSP in terms of the number of commercial deployment of power plant and worldwide installed capacities due to lower initial investment costs involved (Khan and Arsalan, 2016), but CSP is increasingly competing with PV and the number of countries with installed CSP seems to be rapidly growing (Baharoon et al., 2015). A recent report reveals that CSP plant produces greater energy than PV plant for the same nominal power output which suggests that the economic returns of CSP plant is, somehow, greater than a PV plant (Khan and Arsalan, 2016).

Figure 1.1 shows the schematic diagram of a CSP power plant that uses a two-tank direct system. The CSP generates electricity through sunlight which is concentrated by arrays of mirrors (heliostats) to heat a molten salt used as heat

transfer fluid (HTF) in a receiver tube. The heated HTF is stored in the hot tank that could be used during non-sunlight periods by producing a steam which drives a turbine-generator set through heat exchangers. The cooled HTF is pumped and stored into the other tank for a heating cycle, thereafter.

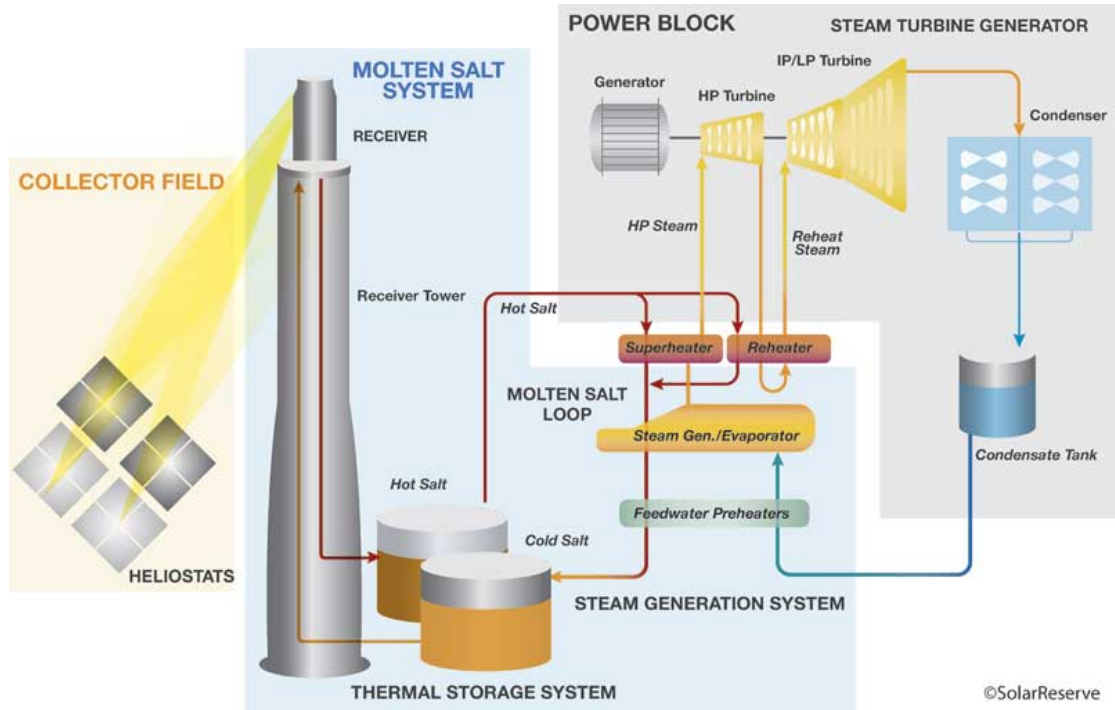


Figure 1.1 Schematic diagram of a CSP power plant (SolarReserve, 2016)

In order to make CSP become more cost-effective, improvement in the capabilities of CSP systems for conversion of sunlight into heat is required. In particular, the thermal storage fluids have been pursued as one of the important subject for R&D in order to improve the energy storage capacity by operating at higher temperature (Lewis, 2016; Kousksou et al., 2014; Baharoon et al., 2015; Liu et al., 2012). Currently, many CSP plants especially the parabolic-trough type use synthetic oil as heat transfer fluid. For high temperature ($> 400\text{ }^{\circ}\text{C}$), replacement of oil is required and molten salt- or metal-based phase change material (PCM) were

identified as excellent candidates since they can operate at high temperature due to their high melting temperature.

For solar energy harvesting, latent-heat-based thermal energy storage (TES) system using PCMs has attracted attention because it offers high thermal storage density in comparison to sensible heat storage devices. Previous work has demonstrated that PCM has the capacity to store more heat per volume (around 3 – 4 times) than sensible heat storage material (Mehling and Cabeza, 2008). PCM relies on phase change occurring between liquid and solid states for energy storage and release in an isothermal process. Salt (carbonates, nitrates etc...) and metallic materials are the candidates for PCMs in solar application due to their high melting point. Compared to metallic materials, salts are cheaper but they exhibit lower thermal conductivity which may limit their application. Enhancement of thermal conductivity is required to achieve high heat charging and discharging rates in the salt-based TES system.

Introduction of materials with high thermal conductivity as filler such as carbon-based nanomaterials has been pursued to deal with this issue. Carbon nanofillers such as flaked graphite (Ge et al., 2014a, 2014b), carbon fibers (Elgafy and Lafdi, 2005; Wang et al., 2011; Fan et al., 2013), CNTs (Ye et al., 2014; Wang et al., 2010a; Fan et al., 2013; Wu et al., 2016) and graphene nanosheets/nanoplatelets (Yavari et al., 2011; Fan et al., 2013; Wu et al., 2016; Yuan et al., 2016) have been tested and studied in the past as potential nanofillers for the enhancement of thermal conductivity in PCMs. These carbon allotropes used as additives are good candidates to enhance the thermal conductivity in PCMs due to their excellent intrinsic thermal conductivity and low density.